

**Regge signatures from CLAS  $\Lambda(1520)$  photoproduction data at forward angles**En Wang,<sup>1,\*</sup> Ju-Jun Xie,<sup>2,1,3,†</sup> and Juan Nieves<sup>1,‡</sup><sup>1</sup>*Instituto de Física Corpuscular (IFIC), Centro Mixto CSIC-Universidad de Valencia, Institutos de Investigación de Paterna, Apartado 22085, E-46071 Valencia, Spain*<sup>2</sup>*Institute of Modern Physics, Chinese Academy of Sciences, Lanzhou 730000, China*<sup>3</sup>*State Key Laboratory of Theoretical Physics, Institute of Theoretical Physics, Chinese Academy of Sciences, Beijing 100190, China*

(Received 13 May 2014; revised manuscript received 9 November 2014; published 5 December 2014)

The  $\gamma p \rightarrow K^+ \Lambda(1520)$  reaction mechanism is investigated within a Regge-effective Lagrangian hybrid approach based on our previous study of this reaction [Phys. Rev. C **89**, 015203 (2014)]. Near threshold and for large  $K^+$  angles, the data from both the Continuous Electron Beam Accelerator Facility large acceptance spectrometer (CLAS) and the laser electron photon beamline at SPring-8 (LEPS) can be successfully described by considering the contributions from the contact,  $t$ -channel  $\bar{K}$  exchange,  $u$ -channel  $\Lambda(1115)$  hyperon pole, and  $s$ -channel nucleon pole and  $N^*(2120)$  resonance contributions. However, for higher energies and forward  $K^+$  angles, systematic discrepancies with data appear, which hint at the possible existence of sizable quark-gluon string mechanism effects. We show how the inclusion of a  $\bar{K}$ -Regge-trajectory exchange in the  $t$  channel leads to an efficient description of the  $\Lambda(1520)$  photoproduction channel over the whole energy and angular ranges accessible in the CLAS experiment.

DOI: [10.1103/PhysRevC.90.065203](https://doi.org/10.1103/PhysRevC.90.065203)

PACS number(s): 13.75.Cs, 14.20.-c, 13.60.Rj

**I. INTRODUCTION**

The associate production of hadrons by photons has been extensively studied because it provides an excellent tool for learning details of the hadron spectrum. In particular, the  $\gamma p \rightarrow K^+ \Lambda(1520)$  reaction is an efficient isospin-1/2 filter for studying nucleon resonances decaying to  $K \Lambda(1520)$ . As a consequence, the experimental database on this reaction has expanded significantly in recent years. In addition to the pioneering measurements at Cornell [1], Cambridge electron accelerator (CEA) [2], Stanford Linear Accelerator Center (SLAC) [3], and Daresbury [4] laboratories, in 2001 the CLAS Collaboration investigated this process in electroproduction [5], and later in 2010 this reaction was examined at photon energies below 2.4 GeV in the LEPS experiment using a forward-angle spectrometer and polarized photons [6,7] and from threshold to 2.65 GeV with the spectrometer arrangement for photon induced reactions (SAPHIR) detector at the electron stretcher facility European Laboratory for Structural Assessment in Bonn [8]. Very recently, the exclusive  $\Lambda(1520)$  photoproduction cross section has been measured by using the CLAS detector for energies from threshold up to an invariant  $\gamma p$  mass  $W = 2.85$  GeV [9].

In parallel to this great experimental activity, there have also been a large number of theoretical investigations of the  $\Lambda(1520)$  ( $\equiv \Lambda^*$ ) resonance production with the  $\gamma p \rightarrow K^+ \Lambda(1520)$  reaction. For invariant masses  $W \leq 3$  GeV, most of these theoretical calculations [10–16] describe reasonably well the experimental data within the framework of the effective Lagrangian approach. One of the latest of these works corresponds to that of Ref. [15], where, in addition

to the contact,  $s$ -channel nucleon pole, and  $t$ -channel  $\bar{K}$  exchange contributions, which were already considered in previous works, the  $s$ -channel  $N^*(2120)$  [previously called  $N^*(2080)$ ] resonance and the  $u$ -channel  $\Lambda(1115)$  hyperon pole terms were also included. The latter mechanism had been ignored in all previous calculations [10,13,14] that relied on the very forward  $K^+$  angular LEPS data [6,7], where its contribution was expected to be small. However, it produced an enhancement for large  $K^+$  angles, and it becomes more and more relevant as the photon energy increases, being essential to describe the CLAS differential cross sections at backward angles. Besides, the combined analysis of the CLAS and LEPS data carried out in Ref. [15] provided further support on the existence of the  $J^P = 3/2^-$   $N^*(2120)$  resonance and additional constraints to its properties, confirming the previous findings of Refs. [13,16]. Indeed, the model of Ref. [15] leads to an overall good description of both sets of data, both at forward and backward  $K^+$  angles and for the whole range of measured  $\gamma p$  invariant masses in the CLAS and LEPS experiments. However, for invariant masses  $W > 2.35$  GeV and forward angles, some small discrepancies (though systematic) between the CLAS data and the theoretical predictions appear (see bottom panels of Fig. 3 of Ref. [15], collected here in the right panels of Fig. 1), which led to a moderate value of the best-fit  $\chi^2/\text{dof} \sim 2.5$ .

This should not be entirely surprising, because the model of Ref. [15] is not suited at high energies and forward angles, where quark-gluon string mechanisms could become important [17–19]. Actually, it is obvious from the analysis of the experimental hadron cross-section data that the Reggeon and the pomeron exchange mechanisms play a crucial role at high energies and small transferred momenta [20,21]. The underlying philosophy of the Regge formalism is as follows. In modeling the reaction amplitude for the  $\gamma p \rightarrow KY$  process at high energies and small  $|t|$  or  $|u|$ , instead of considering the exchange of a finite selection of individual

\*En.Wang@ific.uv.es

†xiejujun@impcas.ac.cn

‡jmnieves@ific.uv.es

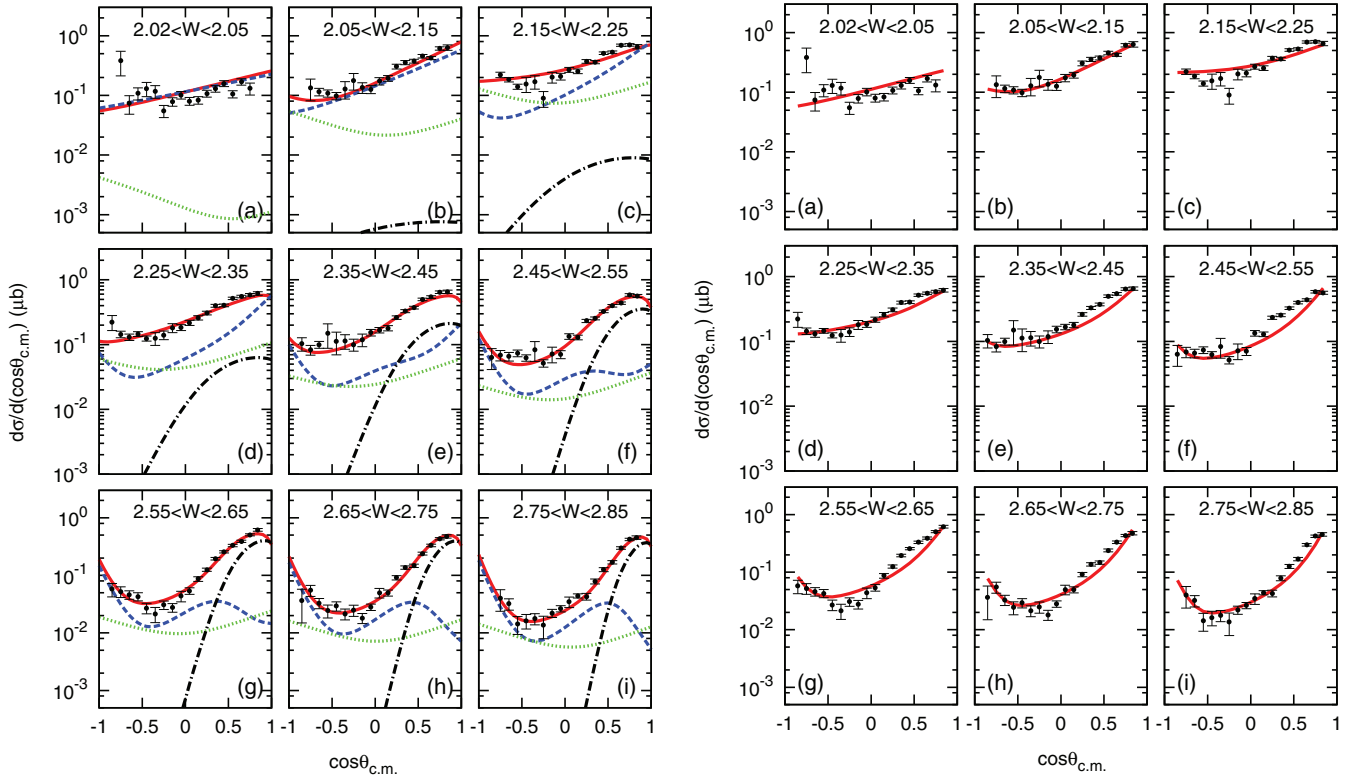


FIG. 1. (Color online) (Left) Model B  $\gamma p \rightarrow K^+ \Lambda(1520)$  differential cross sections as a function of  $\cos\theta_{c.m.}$  compared with the CLAS data [9] for different  $\gamma p$  invariant mass intervals (indicated in the different panels in GeV units). Only statistical errors are displayed. The blue dashed and black dash-dotted curves stand for the contributions from the effective Lagrangian approach background and Reggeon exchange mechanism, respectively (see text for details). The green dotted lines show the contribution of the  $N^*(2120)$  resonance term, while the red solid lines display the results obtained from the full model. (Right) Total results from our previous Fit II carried out in Ref. [15], where Regge effects were not considered.

particles, the exchange of entire Regge trajectories is taken into account. This exchange can take place in the  $t$  channel (kaonic trajectories) or  $u$  channel (hyperonic trajectories). As such, Regge theory offers an elegant way to circumvent the controversial issue of modeling high-spin, high-mass particle exchange.

Different dominant mechanisms have been proposed to describe the large aperture magnet spectrometer (LAMP2), measured at Daresbury laboratory [4] high-energy differential cross sections. Thus, in Refs. [18,19] a large contribution from a  $t$ -channel  $\bar{K}^*$  Regge exchange was claimed. However in Ref. [17], it was argued that the  $\bar{K}^*$  contribution should be quite small, almost negligible, because the  $K^* N \Lambda^*$  coupling is expected to be much smaller than the value implicitly assumed in the previous works.<sup>1</sup> Nevertheless, a Reggeon exchange model, but with a  $\bar{K}$  (instead of a  $\bar{K}^*$ )

trajectory was also used in Ref. [17]. It was also discussed there that the  $\bar{K}$ -Reggeon mechanism is more favored by the LAMP2 data than the  $\bar{K}^*$ -Reggeon one and that it is able to reproduce the available experimental data in the region from  $E_\gamma^{\text{LAB}} \sim 2.8$  GeV up to 5 GeV. Reggeized propagators for the  $\bar{K}$  and  $\bar{K}^*$  exchanges in the  $t$  channel implemented in a gauge-invariant manner were employed in Ref. [23] and compared to Daresbury data. Note, however, that the  $\bar{K}^*$  exchange contribution was also neglected in Ref. [23].

In this work, we aim to correlate the systematic (small) visible discrepancies, at high  $\gamma p$  invariant masses and small angles, among the theoretical predictions of Ref. [15] and the CLAS data with Regge effects. To this end, we improve on the model of Ref. [15] by including the contribution of a  $\bar{K}$ -Regge-trajectory exchange at high energies and low momentum transfers. We use a hybrid model which interpolates from the hadron effective Lagrangian approach, for energies close to threshold, to the quark-gluon string reaction mechanism approach, respecting gauge invariance.

Recently, a work [24] with similar objectives and ideas has appeared. There the crucial role played by the  $u$ -channel  $\Lambda(1115)$  hyperon pole term at backward angles is confirmed, as well as the importance of the  $N^*(2120)$  resonance to describe the LEPS data. Moreover, Regge effects are also

<sup>1</sup>This is because the  $\Lambda(1520)$  resonance is located very close to the threshold energy of the  $\pi \Sigma^*(1385)$  channel, which dominates the  $\Lambda(1520)$  dynamics. Indeed, it could be considered as the bound state of these two hadrons, with some corrections from coupled-channel dynamics. For very small binding energies, all the couplings of the resonance tend to zero as the mass of the bound state approaches the  $\pi \Sigma^*(1385)$  threshold [22].

discussed and taken into account, within a hybrid model that has indeed many formal resemblances with the one presented in this work. However, in contrast with the model derived here,  $\bar{K}^*$  Regge-trajectory effects are considered in Ref. [24] and claimed to provide a considerable contribution at high energies. Furthermore, the couplings of the  $N^*(2120)$  state are fixed to those deduced in the constituent quark model of Refs. [25,26], and a large width of 330 MeV is also set for this resonance. In this way, a great opportunity to take advantage of the accurate LEPS and CLAS data, not only for claiming the existence of the two-star  $N^*(2120)$  state, but also for constraining/determining some of its poorly known properties is somehow missed in the analysis carried out in Ref. [24].

The present paper is organized as follows. In Sec. II, we discuss the formalism and the main ingredients of the model. In Sec. III, we present our main results and, finally, a short summary and conclusions are given in Sec. IV. In the Appendix, we collect results obtained from a different fitting strategy.

## II. FORMALISM AND INGREDIENTS

### A. Feynman amplitudes

Within the effective Lagrangian approach for the  $\Lambda(1520)$  photoproduction reaction,

$$\gamma(k_1, \lambda) p(k_2, s_p) \rightarrow K^+(p_1) \Lambda^*(p_2, s_{\Lambda^*}), \quad (1)$$

the invariant scattering amplitudes are defined as

$$-iT_i = \bar{u}_\mu(p_2, s_{\Lambda^*}) A_i^{\mu\nu} u(k_2, s_p) \epsilon_\nu(k_1, \lambda), \quad (2)$$

where the kinematical variables  $(k_1, k_2, p_1, p_2)$  are defined as in Refs. [13,15], with  $t$ ,  $s$ , and  $u$  the Mandelstam variables:  $t = q_t^2 = (k_1 - p_1)^2$ ,  $s = (k_1 + k_2)^2$ , and  $u = q_u^2 = (p_2 - k_1)^2$ . On the other hand,  $u_\mu$  and  $u$  are dimensionless Rarita-Schwinger and Dirac spinors, respectively, while  $\epsilon_\nu(k_1, \lambda)$  is the photon polarization vector. In addition,  $s_p$  and  $s_{\Lambda^*}$  are the proton and  $\Lambda(1520)$  polarization variables, respectively. The subindex  $i$  stands for the contact,  $t$ -channel antikaon exchange,  $s$ -channel nucleon, and  $N^*(2120)$  ( $\equiv N^*$ ) resonance pole terms (depicted in Fig. 1 of Ref. [13]) and the  $u$ -channel  $\Lambda$  pole mechanism (depicted in Fig. 2 of Ref. [15]). In Eq. (2),  $A_i^{\mu\nu}$  are the reduced tree level amplitudes which can be obtained from the effective Lagrangian densities given in Refs. [13,15]. For the sake of completeness, we also present here these amplitudes (see Refs. [13,15] for some more details):

$$A_t^{\mu\nu} = -e \frac{g_{KN\Lambda^*}}{m_K} \frac{1}{t - m_K^2} q_t^\mu (q_t^\nu - p_1^\nu) \gamma_5 f_c, \quad (3)$$

$$A_s^{\mu\nu} = -e \frac{g_{KN\Lambda^*}}{m_K} \frac{1}{s - m_N^2} p_1^\mu \gamma_5 \left[ \not{k}_1 \gamma^\nu f_s + (\not{k}_2 + m_N) \gamma^\nu f_c \right. \\ \left. + (\not{k}_1 + \not{k}_2 + m_N) i \frac{\kappa_p}{2m_N} \sigma_{\nu\rho} k_1^\rho f_s \right], \quad (4)$$

$$A_c^{\mu\nu} = e \frac{g_{KN\Lambda^*}}{m_K} g^{\mu\nu} \gamma_5 f_c, \quad (5)$$

$$A_R^{\mu\nu} = \gamma_5 \left( \frac{g_1}{m_K} \not{p}_1 g^{\mu\rho} - \frac{g_2}{m_K^2} p_1^\mu p_1^\rho \right) \frac{\not{k}_1 + \not{k}_2 + M_{N^*}}{s - M_{N^*}^2 + i M_{N^*} \Gamma_{N^*}} \\ \times P_{\rho\sigma} \left[ \frac{ef_1}{2m_N} (k_1^\sigma \gamma^\nu - g^{\sigma\nu} \not{k}_1) \right. \\ \left. + \frac{ef_2}{(2m_N)^2} (k_1^\sigma k_2^\nu - g^{\sigma\nu} k_1 \cdot k_2) \right] f_R, \quad (6)$$

$$A_u^{\mu\nu} = \left[ \frac{h_1}{2m_\Lambda} (k_1^\mu \gamma^\nu - g^{\mu\nu} \not{k}_1) + \frac{h_2}{(2m_\Lambda)^2} (k_1^\mu q_u^\nu - g^{\mu\nu} k_1 \cdot q_u) \right] \\ \times \frac{\not{q}_u + m_\Lambda}{u - m_\Lambda^2} g_{KN\Lambda} \gamma_5 f_u. \quad (7)$$

Form factors, needed because the hadrons are not pointlike particles, have been also included in the above expressions. We use the parametrization [27,28]

$$f_i = \frac{\Lambda_i^4}{\Lambda_i^4 + (q_i^2 - M_i^2)^2}, \quad i = s, t, R, u, \quad (8)$$

$$f_c = f_s + f_t - f_s f_t, \quad \text{and} \quad \begin{cases} q_s^2 = q_R^2 = s, \\ M_s = m_N, \\ M_t = m_K, \\ M_R = M_{N^*}, \\ M_u = m_\Lambda, \end{cases} \quad (9)$$

where the form of  $f_c$  is chosen such that the on-shell values of the coupling constants are reproduced and gauge invariance is preserved.

The issue of consistent interactions for off-shell fermion fields of arbitrary spin is addressed in detail in Refs. [29,30]. Our treatment of the Rarita-Schwinger fields is consistent, at least on the mass shell. Nevertheless, the momentum dependence of the interaction in Eq. (6) might lead to unphysical structures in the energy dependence of the cross sections, when the short-distance physics is cut off with a hadronic form factor like the one in Eq. (9) [29]. However, as we will see, for the range of values used in this work for  $\Lambda_R$ , it seems that this problem is not affecting our predictions.

### B. Regge contributions

We base our model on the exchange of a dominant  $\bar{K}$ -Regge trajectory in the  $t$  channel, as suggested in Ref. [17] and corroborated in Ref. [23]. The kaon trajectory represents the exchange of a family of particles with kaon-type internal quantum numbers. We discuss two different models to include the Regge contribution in the present calculation.<sup>2</sup>

- (i) *Model A.* In this case, the kaon Regge trajectory contribution is obtained from the Feynman amplitude  $A_t^{\mu\nu}$  of Eq. (3) by replacing the usual kaon polelike Feynman propagator by a so-called Regge propagator,

<sup>2</sup>We remind the reader that when Reggeized propagators are employed the gauge invariance is broken and that  $t$ -channel Regge effects should only be relevant for forward angles and high energies. These two points are addressed below.

while keeping the rest of the vertex structure, i.e.,

$$\frac{1}{t - m_K^2} \rightarrow \left(\frac{s}{s_0}\right)^{\alpha_K} \frac{\pi \alpha'_K}{\Gamma(1 + \alpha_K) \sin(\pi \alpha_K)}, \quad (10)$$

with  $\alpha_K(t) = \alpha'_K(t - m_K^2) = 0.8 \text{ GeV}^{-2} \times (t - m_K^2)$ , the linear Reggeon trajectory associated to the kaon quantum numbers. The constant  $s_0$  is taken as the Mandelstam variable  $s$  at threshold [ $s_0 = (m_K + M_{\Lambda^*})^2$ ], and it is introduced to fix the dimensions and to normalize the coupling constants. This approach is similar to that followed in Ref. [23], which was also adopted in Ref. [24]. The scattering amplitude for the Reggeon exchange will finally read

$$(A_t^{\mu\nu})^{\text{Regg}} = -e \frac{\bar{g}_{KN\Lambda^*}}{m_K} \frac{q_t^\mu (q_t^\nu - p_1^\nu)}{t - m_K^2} \gamma_5 \mathcal{F}_A^{\text{Regg}}, \quad (11)$$

$$\mathcal{F}_A^{\text{Regg}}(t) = \left(\frac{s}{s_0}\right)^{\alpha_K} \frac{\pi \alpha'_K (t - m_K^2)}{\Gamma(1 + \alpha_K) \sin(\pi \alpha_K)}, \quad (12)$$

where  $\bar{g}_{KN\Lambda^*} = g_{KN\Lambda^*} \times \hat{f}$ , with  $\hat{f}$  a overall normalization factor of the Reggeon exchange contribution. Actually, Reggeon couplings to mesons and baryons might be, in general, different by up to a factor of 2 [21]. This undetermined scale will be fitted to the available data.

Note that the Regge propagator of Eq. (10) has the property that it reduces to the Feynman propagator  $1/(t - m_K^2)$  if one approaches the first pole on the trajectory (i.e.,  $t \rightarrow m_K^2$ , and thus  $\mathcal{F}_A^{\text{Regg}} \rightarrow 1$ ). This means that the farther we go from the pole, the more the result of the Regge model will differ from conventional Feynman-diagram-based models.

- (ii) *Model B.* In the region of negative  $t$ , the Reggeized propagator in Eq. (12) exhibits a factorial growth,<sup>3</sup> which is, in principle, not acceptable [31]. Accordingly, the authors of Refs. [17,21] proposed the use of a form factor that decreased with  $t$  and a simplified expression for the Regge contribution,<sup>4</sup>

$$T_{\text{Regg}} \sim \frac{e \bar{g}_{KN\Lambda^*}}{m_K} \left(\frac{s}{s_0}\right)^{\alpha_K(t)} F(t), \quad (13)$$

with  $F(t)$  a Gaussian form factor that accounts for the compositeness of the external (incoming and outgoing) hadrons,

$$F(t) = e^{t/a^2}, \quad (14)$$

with a typical value of the cutoff parameter  $a \sim 2 \text{ GeV}$ . By analogy with model A, we include in this context the Regge effects by replacing the form factor  $f_c$  in Eq. (3) with

$$f_c \rightarrow \hat{f} \times \mathcal{F}_B^{\text{Regg}} = \hat{f} \times \left(\frac{s}{s_0}\right)^{\alpha_K(t)} e^{t/a^2}. \quad (15)$$

### 1. Considerations on gauge invariance

The inclusion of Regge effects, in either of the two models discussed above, breaks gauge invariance. The amplitudes of the  $s$ -channel  $N^*(2120)$  and the  $u$ -channel  $\Lambda(1115)$  pole mechanisms are gauge invariant by themselves, while some cancellations among the  $t$ -channel  $\bar{K}$  exchange, the  $s$ -channel nucleon-pole, and the contact-term contributions are needed to fulfill gauge invariance. In the  $s$ -channel nucleon pole amplitude, the terms modulated by the form factor  $f_s$  are already gauge invariant. Thus, the cancellations mentioned refer only to the part of the  $T_s$  amplitude affected by the form factor  $f_c$ . We denote this partial amplitude as  $T_s^*$ . Thus, any modification of the  $t$ -channel  $\bar{K}$  exchange mechanism should have an appropriate counterpart in the nucleon-pole and contact-term contributions. To restore gauge invariance, we follow the procedure discussed in Refs. [33,34] and also adopted in Ref. [23] and replace  $(T_t^{\text{Regg}} + T_s^* + T_c)$  with

$$T_t^{\text{Regg}} + (T_s^* + T_c) \times \hat{f} \times \mathcal{F}_{A,B}^{\text{Regg}}. \quad (16)$$

### 2. Hybrid hadron and Reggeon exchange model

We propose a hybrid mechanism to study the  $\gamma p \rightarrow K^+ \Lambda(1520)$  reaction in the range of laboratory photon energies explored by the CLAS Collaboration data. At the lowest invariant masses, near threshold, we consider the effective Lagrangian model of Ref. [15], whose amplitudes were collected in Sec. II A. However, for the higher photon energies ( $W > W_0$ ) and at low momentum transfers ( $|t| < t_0$ ), or equivalently very forward  $K^+$  angles, we assume that the string quark-gluon mechanism, discussed in Sec. II B, is dominant. Here  $W_0$  is a certain value of the  $\gamma p$  invariant mass above which the Regge contribution starts becoming relevant. Similar considerations apply to the Mandelstam variable  $t$ , and its distinctive value  $t_0$ , which limits the kaon scattering angles where the Regge behavior is visible. We implement a smooth transition/interpolation between both reaction mechanisms [17], following the procedure adopted in Ref. [23]. Actually, we define and parametrize this hybrid model by using the invariant amplitudes of Eqs. (3)–(7), but replacing the form factor  $f_c$  with  $\bar{f}_c$ ,

$$f_c \rightarrow \bar{f}_c \equiv \mathcal{F}_{A,B}^{\text{Regg}} \times \hat{f} \times \mathcal{R} + f_c(1 - \mathcal{R}), \quad (17)$$

with

$$\mathcal{R} = \mathcal{R}_W \times \mathcal{R}_t, \quad (18)$$

$$\mathcal{R}_W = \frac{1}{1 + e^{-(W-W_0)/\Delta W}}, \quad (19)$$

$$\mathcal{R}_t = \frac{1}{1 + e^{(|t|-t_0)/\Delta t}}, \quad (20)$$

<sup>3</sup>Note,  $[\Gamma(1 + \alpha_K) \sin(\pi \alpha_K)]^{-1} = \Gamma(1 - \alpha_K) / \pi \alpha_K$ .

<sup>4</sup>In Refs. [17,21], trajectories with a rotating ( $e^{-i\pi \alpha_K(t)}$ ) phase, instead of a constant phase (see, for instance, the discussion in Ref. [32]) were assumed. The difference is an additional factor  $(-1)^{\alpha_K(t)}$  in Eq. (13), which only affects to the interference between the Regge and hadronic contributions. Such interference occurs only in a limited window of  $\gamma p$  invariant masses and  $t$  values, which is not well defined, theoretically. Nevertheless, the CLAS data favor a constant phase as used in Eq. (13).



where we fix  $W_0 = 2.35$  GeV and  $\Delta W = 0.08$  GeV from the qualitative comparison of the predictions of Ref. [15] with the CLAS data and from the findings of Ref. [23]. In addition, we consider  $t_0$  and  $\Delta t$  as free parameters that will be fitted to data.<sup>5</sup> Thus, Regge effects are smoothly incorporated with the variation of  $\mathcal{R}$  from zero to one. The transition from the Regge model to the effective Lagrangian one is controlled by the skin parameters  $\Delta W$  and  $\Delta t$ .

Finally, we note that gauge invariance is accomplished at any value of  $\mathcal{R}$ .

### C. Differential cross section

The unpolarized differential cross section in the center-of-mass (c.m.) frame for the  $\gamma p \rightarrow K^+ \Lambda(1520)$  reaction reads

$$\frac{d\sigma}{d\cos\theta_{c.m.}} = \frac{m_N M_{\Lambda^*} |\vec{k}_1^{c.m.}| |\vec{p}_1^{c.m.}|}{8\pi(s - m_N^2)^2} \sum_{\lambda, s_p, s_{\Lambda^*}} |T|^2, \quad (21)$$

where  $\vec{k}_1^{c.m.}$  and  $\vec{p}_1^{c.m.}$  are the photon and  $K^+$  meson c.m. three-momenta and  $\theta_{c.m.}$  is the  $K^+$  polar scattering angle. The differential cross section  $d\sigma/d(\cos\theta_{c.m.})$  depends on  $W$  and also on  $\cos\theta_{c.m.}$ .

In addition to the three new free parameters ( $t_0$ ,  $\Delta t$ , and  $\hat{f}$ ) introduced to account for Regge effects, the model of Ref. [15] already had nine free parameters: (i) the mass and width ( $M_{N^*}$  and  $\Gamma_{N^*}$ ) of the  $N^*(2120)$  resonance, (ii) the cutoff parameters  $\Lambda_s = \Lambda_t = \Lambda_u \equiv \Lambda_B$  and  $\Lambda_R$ , and (iii) the  $N^*(2120)$  resonance electromagnetic  $\gamma NN^*$  ( $ef_1$ ,  $ef_2$ ) and strong  $N^* \Lambda^* K$  ( $g_1$ ,  $g_2$ ) couplings and the  $\Lambda(1520)$  magnetic  $\gamma \Lambda \Lambda^*$  ( $h_1$ ) one. To reduce the number of best-fit parameters, we have kept unchanged the contribution of the  $u$ -channel  $\Lambda$  pole contribution, and thus we have set the  $\gamma \Lambda \Lambda^*$  coupling to the value obtained in the Fit II of Ref. [15] ( $h_1 = 0.64$ ). This is justified because the contribution of the  $u$ -channel  $\Lambda$  pole term is only important for backward  $K^+$  angles, and the Regge mechanism should only play a certain role at forward angles. In addition, we have also fixed  $\Lambda_B$  to the value of 620 MeV quoted in Ref. [15]. This cutoff parameter also appears in  $T_u$ , and in the definition of the form factor  $f_c$ , which, following Eq. (17), is replaced with  $\tilde{f}_c$  to account for Regge effects at high energies and low momentum transfers.<sup>6</sup>

<sup>5</sup>We refrain from including  $W_0$  and  $\Delta W$  in the fits because the model already contains a large number of free parameters. Indeed, we checked that the inclusion of  $W_0$  and  $\Delta W$  as a free parameters leads to large statistical correlations, which disappear once these two parameters are fixed. Conversely, we also find that if all  $N^*$  resonance properties are frozen to the results obtained in Ref. [15], the transition region  $W_0$  and  $\Delta W$  parameters could now be fitted to the combined CLAS and LEPS data sets, and they turn out to agree with the values of 2.35 and 0.08 GeV assumed above, with a statistical error of around 0.01 GeV. We include  $t_0$  and  $\Delta t$  in the best fit, because the analysis carried out in Ref. [23] considered the old SLAC and LAMP2 data and the recent LEPS measurements, which are not as accurate at backward angles as the newest CLAS cross sections.

<sup>6</sup> $\Lambda_B$  also appears in the definition of the  $f_s$  form factor that affects to some pieces of the  $s$ -channel pole nucleon term. These contributions

are, however, quite small because they are greatly suppressed by  $f_s$ , and do affect very little the best fit.

### III. NUMERICAL RESULTS AND DISCUSSION

We have performed a ten-parameter ( $g_1$ ,  $g_2$ ,  $\Lambda_R$ ,  $ef_1$ ,  $ef_2$ ,  $M_{N^*}$ ,  $\Gamma_{N^*}$ ,  $t_0$ ,  $\Delta t$ , and  $\hat{f}$ )  $\chi^2$  fit to the LEPS [7] and CLAS [9] measurements of  $d\sigma/d(\cos\theta_{c.m.})$ . There is a total of 216 available data (157 points from CLAS and another 59 ones from LEPS, depicted in Figs. 1 and 2, respectively). The systematical errors of the experimental data (11.6% [9] and 5.92% [7], for CLAS and LEPS, respectively) have been added in quadratures<sup>7</sup> to the statistical ones and taken into account in the fits, as done in Ref. [15]. LEPS data lie in the  $K^+$  forward-angle region and were taken below  $E_\gamma = 2.4$  GeV, while the recent CLAS measurements span a much larger  $K^+$  angular and photon energy regions (nine intervals of the  $\gamma p$  invariant mass from the reaction threshold, 2.02 GeV, up to 2.85 GeV).<sup>8</sup>

We have considered two different schemes to include Regge effects (models A and B), as discussed in Sec. II B. Best-fit results are listed in Table I, where we also compile the obtained parameters in our previous work (Fit II of Ref. [15]). For each fit, we also give the predicted  $N^*(2120)$  partial decay width  $\Gamma_{N^* \rightarrow \Lambda^* K}$  (Eq. (18) of Ref. [13]) and the resonance helicity amplitudes (Eqs. (15) and (16) of Ref. [13]) for the positive-charge state.

A  $\chi^2/\text{dof}$  of around 1.3 is obtained for both model A and B fits. This is significantly better than the best-fit value (2.5) obtained in our previous work [15], where Regge effects were not considered. We also see that the effective Lagrangian approach parameters ( $g_1$ ,  $g_2$ ,  $\Lambda_R$ ,  $ef_1$ ,  $ef_2$ ,  $M_{N^*}$ ,  $\Gamma_{N^*}$ ), determined in the new fits carried out in this work, turn out to be in good agreement with those obtained in Ref. [15]. Thus, the conclusions of that reference still hold, in particular those concerning the existence of the two-star  $N^*(2120)$  resonance and its relevance in the CLAS and LEPS  $\gamma p \rightarrow K^+ \Lambda(1520)$  data. Besides, the hybrid model parameters ( $t_0$ ,  $\Delta t$  and  $\hat{f}$ ) turn out to be reasonable from what one would expect by a direct inspection of the CLAS data ( $t_0$ ,  $\Delta t$ ) and previous estimates [17,21]. In Table II of the Appendix, we show results from model A and B fits obtained neglecting the systematic errors, because one might think it was not entirely justified to add them in quadratures to the statistical uncertainties. The conclusions are qualitatively identical, and the new fitted parameters are compatible, within uncertainties, with those given in Table I, but with a larger  $\chi^2/\text{dof} \sim 3.0$ . The worsening of the best fit  $\chi^2/\text{dof}$ , when Regge effects are neglected, turns out to be

are, however, quite small because they are greatly suppressed by  $f_s$ , and do affect very little the best fit.

<sup>7</sup>The CLAS and LEPS collaborations provide neither statistical nor systematic covariance matrices. Given the lack of a more precise input, we assume fully uncorrelated statistical and systematic covariance matrices.

<sup>8</sup>To compute the cross sections in each interval, we always use the corresponding mean value of  $W$ , as in Ref. [15].

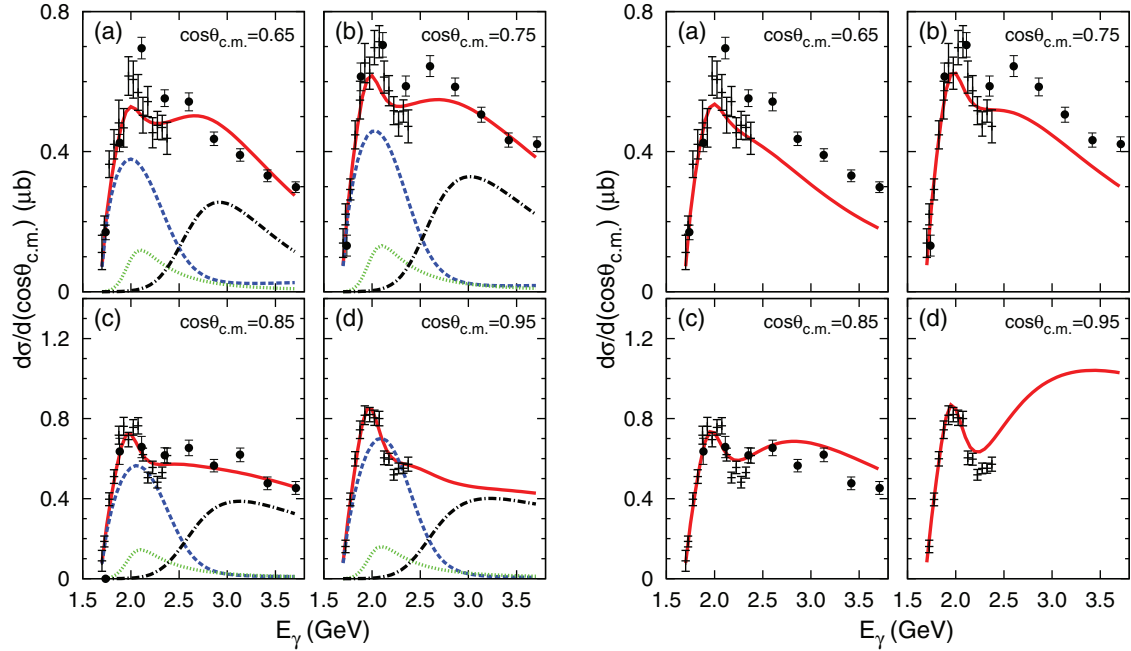


FIG. 2. (Color online) (Left) Model B  $\gamma p \rightarrow K^+ \Lambda(1520)$  differential cross section as a function of the LAB frame photon energy for different c.m.  $K^+$  polar angles. We also show the experimental LEPS [7] (crosses) and CLAS [9] (black dots) data. Only statistical errors are displayed. The blue dashed and black dash-dotted curves stand for the contributions from the effective Lagrangian approach background and Reggeon exchange mechanism, respectively (see text for details). The green dotted lines show the contribution of the  $N^*(2120)$  resonance term, while the red solid lines display the results obtained from the full model. (Right) Total results from our previous Fit II carried out in Ref. [15], where Regge effects were not considered.

more pronounced (see last column of Table II). Yet in this latter case, there appear to be some tensions between the new fitted  $g_2$  and  $\Lambda_R$  parameters and those obtained in the Fit II of Ref. [15].

The fits obtained here are of similar quality to the best ones reported in Ref. [24], where, in addition to the Regge effects driven by kaon exchange in the  $t$  channel, some sizable Regge contributions induced by  $\bar{K}^*$  exchanges are

TABLE I. Values of some parameters determined in this work and in Ref. [15]. Model A (B) parameters have been adjusted to the combined LEPS [7] and CLAS [9]  $\gamma p \rightarrow K^+ \Lambda(1520)$   $d\sigma/d(\cos\theta_{c.m.})$  data including Regge effects as discussed in Eq. (12) [Eq. (15)]. In the last column, we compile some results from Fit II of Ref. [15], where the mechanism of Reggeon exchange was not considered. Finally, we also give for each fit the predicted  $N^*(2120)$  width  $\Gamma_{N^* \rightarrow \Lambda^* K}$  and the helicity amplitudes for the positive-charge  $N^*$  state.

	This work		Ref. [15]
	Model A	Model B	Fit II
$g_1$	$1.3 \pm 0.2$	$1.4 \pm 0.2$	$1.6 \pm 0.2$
$g_2$	$0.9 \pm 0.5$	$1.1 \pm 0.5$	$2.2 \pm 0.5$
$\Lambda_R$ (MeV)	$1252 \pm 78$	$1259 \pm 76$	$1154 \pm 47$
$ef_1$	$0.134 \pm 0.016$	$0.123 \pm 0.015$	$0.126 \pm 0.012$
$ef_2$	$-0.110 \pm 0.014$	$-0.100 \pm 0.013$	$-0.097 \pm 0.010$
$M_{N^*}$ (MeV)	$2146 \pm 5$	$2145 \pm 5$	$2135 \pm 4$
$\Gamma_{N^*}$ (MeV)	$174 \pm 14$	$171 \pm 13$	$184 \pm 11$
$t_0$ (GeV <sup>2</sup> )	$0.73 \pm 0.04$	$0.94 \pm 0.05$	—
$\Delta t$ (GeV <sup>2</sup> )	$0.28 \pm 0.02$	$0.30 \pm 0.04$	—
$\hat{f}$	$0.38 \pm 0.01$	$0.37 \pm 0.01$	—
$\chi^2/\text{dof}$	1.3	1.3	2.5
		Derived observables	
$A_{1/2}^{p^*}$ ( $10^{-3}$ GeV <sup>-1/2</sup> )	$-9.7 \pm 4.1$	$-8.8 \pm 3.8$	$-7.3 \pm 3.0$
$A_{3/2}^{p^*}$ ( $10^{-2}$ GeV <sup>-1/2</sup> )	$2.3 \pm 1.1$	$2.1 \pm 1.0$	$2.5 \pm 0.8$
$\Gamma_{N^* \rightarrow \Lambda^* K}$ (MeV)	$22 \pm 7$	$25 \pm 7$	$30 \pm 8$
$\frac{\Gamma_{N^* \rightarrow \Lambda^* K}}{\Gamma_{N^*}}$ (%)	$12.9 \pm 3.9$	$14.8 \pm 4.5$	$16.2 \pm 4.2$

TABLE II. Model A and B fits, as in Table I, but taking into account only the statistical uncertainties in the LEPS and CLAS data sets. In the last column, we give results obtained when the mechanism of Reggeon exchange is not considered. Finally, we also give for each fit the predicted  $N^*(2120)$  partial decay width  $\Gamma_{N^* \rightarrow \Lambda^* K}$  and the helicity amplitudes for the positive-charge  $N^*$  state.

	Model A	Model B	No Regge
$g_1$	$1.56 \pm 0.09$	$1.40 \pm 0.13$	$1.50 \pm 0.12$
$g_2$	$1.88 \pm 0.59$	$1.69 \pm 0.43$	$4.42 \pm 0.41$
$\Lambda_R$ (MeV)	$1134 \pm 57$	$1160 \pm 49$	$1037 \pm 20$
$ef_1$	$0.123 \pm 0.001$	$0.131 \pm 0.010$	$0.129 \pm 0.007$
$ef_2$	$-0.103 \pm 0.003$	$-0.110 \pm 0.009$	$-0.099 \pm 0.006$
$M_{N^*}$ (MeV)	$2146 \pm 4$	$2146 \pm 4$	$2138 \pm 3$
$\Gamma_{N^*}$ (MeV)	$181 \pm 10$	$175 \pm 10$	$182 \pm 8$
$t_0$ (GeV <sup>2</sup> )	$0.70 \pm 0.02$	$0.92 \pm 0.03$	—
$\Delta t$ (GeV <sup>2</sup> )	$0.30 \pm 0.01$	$0.33 \pm 0.02$	—
$\hat{f}$	$0.38 \pm 0.01$	$0.37 \pm 0.01$	—
$\chi^2/\text{dof}$ (no $\sigma_{\text{sys}}$ )	3.0	3.0	8.4
		Derived observables	
$A_{1/2}^{p*}$ ( $10^{-3} \text{ GeV}^{-1/2}$ )	$-9.5 \pm 0.7$	$-10.0 \pm 2.5$	$-7.5 \pm 0.7$
$A_{3/2}^{p*}$ ( $10^{-2} \text{ GeV}^{-1/2}$ )	$2.0 \pm 0.1$	$2.2 \pm 0.6$	$2.5 \pm 0.2$
$\Gamma_{N^* \rightarrow \Lambda^* K}$ (MeV)	$33 \pm 4$	$27 \pm 5$	$27 \pm 5$
$\frac{\Gamma_{N^* \rightarrow \Lambda^* K}}{\Gamma_{N^*}}$ (%)	$18.1 \pm 2.6$	$15.2 \pm 3.0$	$16.3 \pm 2.2$

included as well. However, as mentioned in the Introduction, theoretically it is difficult to accommodate a  $\bar{K}^*$  mechanism contribution as large as that claimed in Ref. [24] (see Secs. 3.1 and 3.2 of this latter reference). In addition, a bunch of  $N^*$  resonances are included in the approach followed in Ref. [24]. Their couplings and masses are, in most cases, fixed to the constituent quark model predictions of Refs. [25,26] and a common width of 330 MeV is assumed for all of them. Among all of them, it turns out to be the  $N^*(2120)$ , the state that provides the most important contribution, which confirms previous claims [13,14]. We have adopted a different point of view and have used the accurate CLAS and LEPS  $\gamma p \rightarrow K^+ \Lambda(1520)$  data not only to claim the existence of the  $N^*(2120)$  resonance, but also to establish some of its properties. Thus, we find a much narrower state ( $\Gamma_{N^*} \sim 170\text{--}175$  MeV) and complete different helicity amplitudes. Moreover, the values used in Ref. [24] ( $A_{1/2}^{p*} = 36$  and  $A_{3/2}^{p*} = -43$  in [ $10^{-3} \text{ GeV}^{-1/2}$ ] units) are incompatible with both

$$A_{1/2}^{p*} (10^{-3} \text{ GeV}^{-1/2}) = 125 \pm 45, \quad (22)$$

$$A_{3/2}^{p*} (10^{-2} \text{ GeV}^{-1/2}) = 15 \pm 6, \quad (23)$$

given in Ref. [35], and with previous measurements [36],

$$A_{1/2}^{p*} (10^{-3} \text{ GeV}^{-1/2}) = -20 \pm 8, \quad (24)$$

$$A_{3/2}^{p*} (10^{-2} \text{ GeV}^{-1/2}) = 1.7 \pm 1.1, \quad (25)$$

quoted in the 2008 PDG edition [37], that, in turn, are in quite good agreement with our predictions in Table I. Having improved the quality of our fit, achieving now an accurate description of the CLAS data for all angles and invariant mass windows (see below), our results give an important support to the measurements of Ref. [36], which do not seem entirely consistent with those reported in Ref. [35]. Given the two-star status (evidence of existence is only fair) granted

to the  $N^*(2120)$  resonance in the multichannel partial-wave analysis of pion and photoinduced reactions off protons carried out in Ref. [35], the discrepancy with our predicted helicity amplitudes should not be used to rule out our fits, but rather one should interpret our results as further constrains on these elusive observables. Note that the helicity amplitudes given in Eqs. (24) and (25) were also used in Ref. [16], where the  $ep \rightarrow eK^+ \Lambda(1520)$  CLAS data of Ref. [5] were successfully described.

In addition, there is a disturbing feature in the fits presented in Ref. [24]. There it is found that  $t_0 \sim 3 \text{ GeV}^2$ , though with a large error, while we obtain values in the range  $0.7\text{--}0.9 \text{ GeV}^2$ . A value of  $t_0$  as high as  $3 \text{ GeV}^2$  necessarily changes the meaning of the interpolating function  $\mathcal{R}_t$  in Eq. (20), because it will not effectively filter now forward angles. This is easily understood if one realizes that for  $W = 2.4 \text{ GeV}$ ,  $|t|$  remains below  $2.5 \text{ GeV}^2$  for all possible  $K^+$  c.m. angles, and for the highest invariant mass  $W = 2.8 \text{ GeV}$  the bound  $t = -3 \text{ GeV}^2$  is reached for  $\cos \theta_{\text{c.m.}} = -0.3$ . Thus, in the scheme employed in Ref. [24], the transition function  $\mathcal{R}_t$  effectively modifies the predictions of the effective Lagrangian approach, allowing for some Regge effects for large scattering angles, which seems quite doubtful. Probably, this dysfunction of the physical meaning of  $\mathcal{R}_t$  could be a consequence of the unnecessary complexity of the scheme used in Ref. [24] with various  $N^*$  contributions and the inclusion of  $\bar{K}^*$  driven effects, with parameters in some cases fixed to values with little theoretical and experimental support. Nevertheless, it should be acknowledged that the work of Ref. [24] is pioneer in exploring the possible existence of Regge effects in the CLAS data.

The differential  $d\sigma/d(\cos \theta_{\text{c.m.}})$  distributions calculated with the model B best-fit parameters are shown in Figs. 1 and 2 as a function of  $\cos \theta_{\text{c.m.}}$  and for various  $\gamma p$  invariant mass intervals. Model A results are totally similar and, for brevity, they are not discussed any further. Only statistical

errors are displayed in these two figures and the contributions from different mechanisms are shown separately. Thus, we split the full result into three main contributions: effective Lagrangian approach background, Reggeon exchange, and resonance  $N^*(2120)$ . The first one corresponds to the  $t$ -channel  $\bar{K}$  exchange, nucleon pole, contact, and  $u$ -channel  $\Lambda(1115)$  hyperon pole terms of Eqs. (3)–(5) and (7), but evaluated with the modified form factor  $f_c(1 - \mathcal{R})$  instead of  $f_c$ , as discussed in Eq. (17). [Note that  $f_c$  appears neither in the  $\Lambda(1115)$  nor in the resonance  $N^*(2120)$  mechanisms because both of them are gauge invariant by themselves]. The Reggeon contribution is calculated from the  $f_c$  terms of the  $\bar{K}$  exchange, nucleon pole, and contact terms of Eqs. (3)–(5) and (7), but now evaluated with the generalized Regge form factor  $\mathcal{F}_B^{\text{Regg}} \hat{f}\mathcal{R}$ .

In the left panels of the first of these two figures, we show our predictions and the data of the CLAS collaboration [9]. In the right panels and for comparison purposes, we display the final results from our previous Fit II carried out in Ref. [15], where Regge effects were not considered. We find an overall good description of the data for the whole range of measured  $\gamma p$  invariant masses and it is significantly better than that exhibited in the right panels. We see that the Regge improved model provides now an excellent description of the CLAS data for values of  $\cos\theta_{\text{c.m.}}$  above 0.5, and high energies,  $W \geq 2.3$  GeV, as expected. However, by construction, Regge contributions effectively disappear at low invariant masses  $W < 2.3$  GeV and backward  $K^+$  angles. Thus, we recover for this latter kinematics the effective Lagrangian approach, including resonance  $N^*(2120)$  and hyperon  $\Lambda(1115)$  contributions, which successfully described the data in this region [15].

In the left panels of Fig. 2, the differential cross section deduced from the results of the model B fit, as a function of the LAB frame photon energy and for different forward c.m.  $K^+$  angles, is shown and compared both to LEPS [7] and CLAS [9] data sets. In the right panels and for the sake of clarity, we display the final results from our previous Fit II carried out in Ref. [15], where Regge effects were not considered. We see the description of LEPS data is almost not affected by the Regge contributions, and the bump structure in the differential cross section at forward  $K^+$  angles is fairly well described, thanks to the significant contribution from the  $N^*$  resonance in the  $s$  channel, as pointed out in Refs. [13,15]. However, the inclusion of Regge effects significantly improves the description of the CLAS data,<sup>9</sup> as one would expect from the discussion of the results of Fig. 1. Moreover, the hybrid model presented in this work provides a better energy behavior for the forward cross section at energies higher than those explored by the CLAS data [see the two (d) panels in Fig. 2].

Figure 3 shows the  $\Lambda(1520)$  total photoproduction cross section as a function of the photon energy. There, we see (green dotted line) that the  $N^*$  contribution peaks around 2.1 GeV, not showing any pathology [29] that could have been induced by the use of the naive form factor of Eq. (9). This is probably

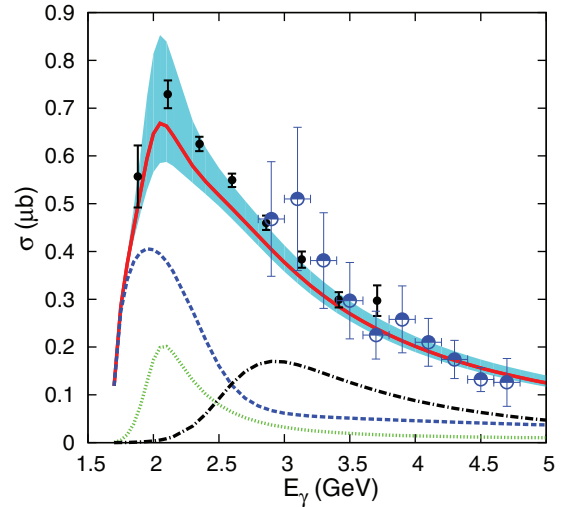


FIG. 3. (Color online) Total  $\gamma p \rightarrow K^+ \Lambda^*$  cross section as a function of the photon energy. Black solid circles and blue open circles stand for CLAS [9] and LAMP2 [4] data, respectively. LAMP2 cross sections have been scaled down by a factor 0.6. Results from model B are also shown. The blue dashed and black dash-dotted curves stand for the contributions from the effective Lagrangian approach background and Reggeon exchange mechanism, respectively (see text for details). The green dotted lines show the contribution of the  $N^*(2120)$  resonance term, while the red solid lines display the results obtained from the full model. The shaded region accounts for the 68% CL band inherited from the Gaussian correlated statistical errors of the parameters.

because we are dealing just with a spin-3/2 resonance, because the effects become larger for higher spins, and, alternatively, to the relatively small value for  $\Lambda_R$  found in the fit [29]. Paying attention now to the data, we see that, despite the overall normalization of the CLAS<sup>10</sup> measurements, Ref. [9] is in rather strong disagreement with the data from LAMP2 [4]; the photon energy dependence of both data sets seems compatible above 2.3 or 2.4 GeV. This can be appreciated in Fig. 3, where the LAMP2 cross sections have been scaled down by a factor 0.6. This agreement might give some support to the idea of finding Regge signatures in the CLAS data. Results from model B are also shown, which turn out to provide a good description of both sets of data. We should, however, inform the reader about the *ad hoc* modification of the normalization of the old LAMP2 cross sections.<sup>11</sup> Nevertheless, it is reassuring that the hybrid model presented in this work, including Regge effects, is able to predict the photon energy dependence of the LAMP2 data at energies well above those explored by the CLAS data.

<sup>9</sup>The CLAS cross sections shown in the figure were obtained from the appropriate CLAS measurements displayed in Fig. 1, relating  $W$  to the LAB photon energy.

<sup>10</sup>We display extrapolated total cross sections, from data summed over the useful acceptance of the detector to  $4\pi$  (red points in Fig. 11 of Ref. [9]).

<sup>11</sup>The low-energy SAPHIR data [8] is in even in a stronger disagreement with the data from LAMP2, with the CLAS results lying almost exactly between these two measurements [9].



#### IV. CONCLUSIONS

We have presented some evidence of Regge signatures in the CLAS data at forward angles, despite that the energies involved in that experiment are only moderately high. This is not entirely surprising because above  $E_\gamma > 2.3\text{--}2.4$  GeV, and up to an overall normalization, the CLAS  $\Lambda(1520)$  total cross-section dependence on the photon energy matches that inferred from the LAMP2 data, which extends up to 5 GeV, in a region where the Regge behavior is expected to be visible (see Fig. 3). Indeed, we find a significant improvement on the description of the CLAS high-energy forward cross sections, when the effective Lagrangian approach of Ref. [15] is supplemented with some string quark-gluon mechanism contributions determined by a kaon trajectory. Now there are no visible systematic discrepancies between the hybrid approach predictions and the data. Thus, we confirm the findings of the recent work of Ref. [24] on the importance of the Regge effects in achieving an accurate description of the CLAS forward angular distributions.

We do not need to include any contribution from a  $\bar{K}^*$  trajectory, in accordance with the analysis of the LAMP2 data carried out in Refs. [17,23]. This might be also in congruence with a small, almost negligible,  $t$ -channel  $\bar{K}^*$  meson contribution. Large values for the  $g_{K^*N\Lambda^*}$  coupling are completely ruled out by unitarized chiral models [17,38,39] and by measurements of the photon-beam asymmetry, as discussed in Ref. [23]. However, a trajectory represents a collection of connected mesons and a coupling strength to a trajectory should not be confused with one to an individual meson.

We have designed a gauge-invariant hybrid model which smoothly interpolates from the hadron effective Lagrangian approach [15], at energies close to threshold, to a model that incorporates quark-gluon string reaction mechanism contributions at high energies and forward  $K^+$  scattering angles. We find an accurate description of both CLAS and LEPS data. The latter set of low-energy cross sections is not affected by the inclusion of Regge effects. The bump structure observed at forward  $K^+$  angles in these data is well described thanks to the significant contribution from the two-star  $J^P = 3/2^-$   $N^*(2120)$  resonance in the  $s$  channel, whose existence gets a stronger support from this improved analysis that is now fully consistent with the accurate CLAS data. Thus, this associated strangeness production reaction becomes an excellent tool to determine the properties of this resonance (helicity amplitudes

determined by the couplings  $ef_1$  and  $ef_2$  or the strength of the  $K\Lambda^*N^*$  vertex). Nevertheless, though encouraging and promising, the statistical significance of the present analysis and of that carried out in Ref. [15] is not totally conclusive and it does not reach the discovery status in what respects to the  $N^*(2120)$  state. With respect to the CLAS data, Regge effects play a crucial role at forward angles for energies above 2.35 GeV, as commented before, while the backward angle data highlight the importance of the  $u$ -channel  $\Lambda(1115)$  hyperon pole term. This latter fact can be used to constrain the radiative  $\Lambda^* \rightarrow \Lambda\gamma$  decay, as it was first emphasized in Ref. [15].

The  $t$  range explored by the CLAS data is not large enough to fully restrict the Regge form factor, which is the major difference among the two models (A and B) introduced in this work. Though in the region of negative  $t$ , the Reggeized propagator in Eq. (12) exhibits a factorial growth, which is, in principle, not acceptable; the limited range of momentum transfers accessible in the data does not see this unwanted behavior. This is the same reason why the Gaussian cutoff parameter  $a$  in Eq. (14) is not further constrained. Unfortunately, the existing large discrepancies among CLAS and LAMP2 data sets prevent the inclusion of this latter experiment in the analysis carried out in this work. This constitutes an open problem, which might require new dedicated experiments.

#### ACKNOWLEDGMENTS

This work was partly supported by DGI and FEDER funds, under Contracts No. FIS2011-28853-C02-01 and No. FIS2011-28853-C02-02, the Spanish Ingenio-Consolider 2010 Program CPAN (Grant No. CSD2007-00042), Generalitat Valenciana under Contract No. PROMETEO/2009/0090, and the National Natural Science Foundation of China under Grant No. 11105126. We acknowledge the support of the European Community-Research Infrastructure Integrating Activity Study of Strongly Interacting Matter (HadronPhysics3, Grant Agreement No. 283286) under the Seventh Framework Programme of the E.U.

#### APPENDIX: FITS CONSIDERING ONLY STATISTICAL ERRORS

In this appendix, we show results (Table II) from model A and B fits obtained neglecting the systematic errors.

- 
- [1] N. Mistry, S. Mori, D. Sober, and A. Sadoff, *Phys. Lett. B* **24**, 528 (1967).
  - [2] W. Blanpied, J. Greenberg, V. Hughes, P. Kitching, and D. Lu, *Phys. Rev. Lett.* **14**, 741 (1965).
  - [3] A. M. Boyarski *et al.*, *Phys. Lett. B* **34**, 547 (1971).
  - [4] D. P. Barber, J. B. Dainton, L. C. Y. Lee, R. Marshall, J. C. Thompson, D. T. Williams, T. J. Brodbeck, G. Frost *et al.*, *Z. Phys. C* **7**, 17 (1980).
  - [5] S. P. Barrow *et al.* (CLAS Collaboration), *Phys. Rev. C* **64**, 044601 (2001).
  - [6] N. Muramatsu *et al.* (LEPS Collaboration), *Phys. Rev. Lett.* **103**, 012001 (2009).
  - [7] H. Kohri *et al.* (LEPS Collaboration), *Phys. Rev. Lett.* **104**, 172001 (2010).
  - [8] F. W. Wieland, J. Barth, K. H. Glander, J. Hannappel, N. Jopen, F. Klein, E. Klempt, R. Lawall *et al.*, *Eur. Phys. J. A* **47**, 47 (2011); **47**, 133 (2011).
  - [9] K. Moriya *et al.* (CLAS Collaboration), *Phys. Rev. C* **88**, 045201 (2013).
  - [10] S.-I. Nam, A. Hosaka, and H.-C. Kim, *Phys. Rev. D* **71**, 114012 (2005).

- [11] S.-I. Nam, K.-S. Choi, A. Hosaka, and H.-C. Kim, *Phys. Rev. D* **75**, 014027 (2007).
- [12] S.-I. Nam, *Phys. Rev. C* **81**, 015201 (2010).
- [13] J.-J. Xie and J. Nieves, *Phys. Rev. C* **82**, 045205 (2010).
- [14] J. He and X.-R. Chen, *Phys. Rev. C* **86**, 035204 (2012).
- [15] J.-J. Xie, E. Wang, and J. Nieves, *Phys. Rev. C* **89**, 015203 (2014).
- [16] S.-I. Nam, *J. Phys. G* **40**, 115001 (2013).
- [17] H. Toki, C. García-Recio, and J. Nieves, *Phys. Rev. D* **77**, 034001 (2008).
- [18] A. I. Titov, B. Kämpfer, S. Daté, and Y. Ohashi, *Phys. Rev. C* **72**, 035206 (2005); **72**, 049901(E) (2005); **74**, 055206 (2006).
- [19] A. Sibirtsev, J. Haidenbauer, S. Krewald, U.-G. Meißner, and A. W. Thomas, *Eur. Phys. J. A* **31**, 221 (2007).
- [20] A. Donnachie and P. V. Landshoff, *Phys. Lett. B* **185**, 403 (1987).
- [21] V. Y. Grishina, L. A. Kondratyuk, W. Cassing, M. Mirazita, and P. Rossi, *Eur. Phys. J. A* **25**, 141 (2005).
- [22] S. Weinberg, *Phys. Rev.* **137**, B672 (1965).
- [23] A.I. Titov, B. Kämpfer, S. Date, and Y. Ohashi, *Phys. Rev. C* **81**, 055206 (2010).
- [24] J. He, *Nucl. Phys. A* **927**, 24 (2014).
- [25] S. Capstick, *Phys. Rev. D* **46**, 2864 (1992).
- [26] S. Capstick and W. Roberts, *Phys. Rev. D* **58**, 074011 (1998).
- [27] H. Haberzettl, C. Bennhold, T. Mart, and T. Feuster, *Phys. Rev. C* **58**, R40(R) (1998).
- [28] R. M. Davidson and R. Workman, *Phys. Rev. C* **63**, 025210 (2001).
- [29] T. Vrancx, L. De Cruz, J. Ryckebusch, and P. Vancraeyveld, *Phys. Rev. C* **84**, 045201 (2011).
- [30] G. Vereshkov and N. Volchanskiy, *Phys. Rev. C* **87**, 035203 (2013).
- [31] W. Cassing, L. A. Kondratyuk, G. I. Lykasov, and M. V. Ryzanin, *Phys. Lett. B* **513**, 1 (2001).
- [32] M. Guidal, J. M. Laget, and M. Vanderhaeghen, *Nucl. Phys. A* **627**, 645 (1997).
- [33] T. Corthals, J. Ryckebusch, and T. Van Cauteren, *Phys. Rev. C* **73**, 045207 (2006).
- [34] T. Corthals, T. Van Cauteren, J. Ryckebusch, and D. G. Ireland, *Phys. Rev. C* **75**, 045204 (2007).
- [35] A. V. Anisovich, R. Beck, E. Klempt, V. A. Nikonov, A. V. Sarantsev, and U. Thoma, *Eur. Phys. J. A* **48**, 15 (2012).
- [36] R. Kajikawa, eConf C **810824**, 352 (1981).
- [37] C. Amsler *et al.* (Particle Data Group Collaboration), *Phys. Lett. B* **667**, 1 (2008).
- [38] T. Hyodo, S. Sarkar, A. Hosaka, and E. Oset, *Phys. Rev. C* **73**, 035209 (2006); **75**, 029901 (2007).
- [39] D. Gamermann, C. Garcia-Recio, J. Nieves, and L. L. Salcedo, *Phys. Rev. D* **84**, 056017 (2011).